Chapter 2
Neutrinos and Weak Interactions in the Standard Model

Abstract Neutrinos are produced and detected by weak interactions. It is necessary to understand the weak interactions to calculate the energy spectrum of neutrinos generated in sources and the reaction cross section with detector materials. In this chapter, the weak interactions associated with the neutrinos are reviewed and neutrino reaction probabilities that will be used in the later sections are calculated. Starting from the wave function of the massless left-handed neutrinos, the neutrino-associated parts of the standard model Lagrangian are introduced. Based on the Lagrangian, the general matrix element for the four fermion interactions that include neutrino is formulated. The spectra of neutrinos produced in the pion decay, muon decay, β decay, and the neutrino detection cross section via νe elastic scatterings and inverse beta decay are quantitatively calculated.

Keywords Standard model · Weak interaction · Helicity · Neutrino source · Neutrino interaction

2.1 Introductions

In order to investigate the neutrino oscillation in experiments, we need to understand the properties and the reactions of neutrinos qualitatively within the standard model. In planning experiments and understanding their data, the production mechanism of neutrinos and its reaction cross sections with matter are particularly important. In this chapter we focus on the weak interactions that are related to the neutrino reactions based on the Lagrangian which is summarized in Sect. 8.2.

2.2 Quarks, Charged Leptons and Neutrinos

In the standard model of elementary particles, the six fermions which couple to the strong interactions are called *quarks*

$$\begin{pmatrix} u \\ d \end{pmatrix}, \quad \begin{pmatrix} c \\ s \end{pmatrix}, \quad \begin{pmatrix} t \\ b \end{pmatrix}, \tag{2.1}$$

F. Suekane, *Neutrino Oscillations*, Lecture Notes in Physics 898,
DOI 10.1007/978-4-431-55462-2_2

where u, c, t quarks have charge $+2/3$ and d, s, b quarks have charge $-1/3$ in the unit of e. The six fermions which do not couple to the strong interactions are called the *leptons*

$$\begin{pmatrix}\nu_e\\ e^-\end{pmatrix},\quad \begin{pmatrix}\nu_\mu\\ \mu^-\end{pmatrix},\quad \begin{pmatrix}\nu_\tau\\ \tau^-\end{pmatrix}. \tag{2.2}$$

The ν_e, ν_μ and ν_τ do not couple to the electromagnetic interactions and are called *neutrinos*. The e, μ and τ have the electric charge -1 and are called *charged leptons*. All the fermions have their antiparticles,[1]

$$\begin{pmatrix}\overline{u}\\ \overline{d}\end{pmatrix},\quad \begin{pmatrix}\overline{c}\\ \overline{s}\end{pmatrix},\quad \begin{pmatrix}\overline{t}\\ \overline{b}\end{pmatrix},\quad \begin{pmatrix}\overline{\nu}_e\\ e^+\end{pmatrix},\quad \begin{pmatrix}\overline{\nu}_\mu\\ \mu^+\end{pmatrix},\quad \begin{pmatrix}\overline{\nu}_\tau\\ \tau^+\end{pmatrix}. \tag{2.3}$$

As for the interactions, the electromagnetic interactions are mediated by the massless spin-1 photon

$$\gamma. \tag{2.4}$$

The weak interactions are mediated by the massive spin-1 charged and neutral bosons,

$$W^\pm,\quad Z^0. \tag{2.5}$$

The strong interactions are mediated by the massless spin-1 vector boson called gluon,

$$g. \tag{2.6}$$

Finally the Higgs field generates the fermion and weak boson masses.

$$H^0. \tag{2.7}$$

The three interactions have a nesting structure, illustrated as a Matryoshka doll in Fig. 2.1. The fermions that feel the EM interactions also feel the weak interactions. Fermions that feel the strong interactions also feel the EM interactions and therefore feel the weak interactions.

What makes the standard model neutrinos unique is that the neutrinos do not feel the electromagnetic, strong, nor gravitational interactions. In other words, the neutrinos are chargeless, colorless and massless particles.

$$Q_\nu = 0,\quad g_S^\nu = 0,\quad m_\nu = 0. \tag{2.8}$$

Only left-handed (LH) neutrinos and right-handed (RH) antineutrinos couple to the weak bosons. Therefore, it can be regarded that there are only LH neutrinos or RH antineutrinos in our world.

$$\nu_L,\quad \overline{\nu}_R. \tag{2.9}$$

The LH and RH denote helicity states which will be explained in the next subsection.

[1] Neutrinos are treated as Dirac particle in this book unless otherwise specified.

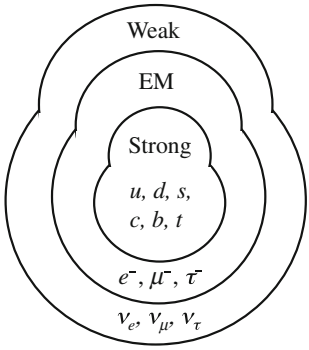

Fig. 2.1 Fermions are named based on the interactions they feel. There is a nesting structure of interactions like a Matryoshka doll

2.2.1 Wave Function of Fermions

The wave function of a spin 1/2 fermion can be obtained as the solution of the Dirac equation,

$$\left[i\gamma_\mu \partial^\mu - m\right]\psi = 0, \tag{2.10}$$

where γ_μ are 4×4 matrices called *gamma matrices* or *Dirac matrices*.

We use the Dirac representation,

$$\gamma_0 = \begin{pmatrix} I & 0 \\ 0 & -I \end{pmatrix}, \quad \gamma_k = \begin{pmatrix} 0 & \sigma_k \\ -\sigma_k & 0 \end{pmatrix}. \tag{2.11}$$

I is the identity matrix and σ_k are the Pauli matrices,

$$I = \begin{pmatrix} 1 & 0 \\ 0 & 1 \end{pmatrix}, \quad \sigma_x = \begin{pmatrix} 0 & 1 \\ 1 & 0 \end{pmatrix}, \quad \sigma_y = \begin{pmatrix} 0 & -i \\ i & 0 \end{pmatrix}, \quad \sigma_z = \begin{pmatrix} 1 & 0 \\ 0 & -1 \end{pmatrix}. \tag{2.12}$$

From Sect. 8.4, the plane wave solution of the Dirac equation with normalization $|\psi|^2 = 2E$ is

$$\psi(x) = \sqrt{E+m}\left[\begin{pmatrix} \hat{u} \\ (\eta \cdot \sigma)\hat{u} \end{pmatrix} e^{-ipx} + \begin{pmatrix} (\eta \cdot \sigma)\hat{v} \\ \hat{v} \end{pmatrix} e^{ipx}\right]; \quad \eta = \frac{\mathbf{p}}{E+m}, \tag{2.13}$$

where $p = (E, \mathbf{p})$ is the four momentum and $E = \sqrt{\mathbf{p}^2 + m^2}$ is the energy. $\hat{u}$ and $\hat{v}$ are two component spinors with the normalization of $|\hat{u}|^2 + |\hat{v}|^2 = 1$, which represent the spin direction. The first term of (2.13) is the positive energy state and the second term is the negative energy state that corresponds to the antiparticle.

2.2.1.1 Helicity and Spin Direction

The charged weak boson, $W^{\pm}$ couples only to the left-handed fermions. The left-handed (LH) and right-handed (RH) components of a state ψ are defined by

$$\begin{aligned} \psi_{\mathrm{L}} &\equiv \gamma_L \psi \equiv \frac{1-\gamma_5}{2}\psi = \frac{1}{2}\begin{pmatrix} I & -I \\ -I & I \end{pmatrix}\psi \\ \text{and } \psi_{\mathrm{R}} &\equiv \gamma_R \psi \equiv \frac{1+\gamma_5}{2}\psi = \frac{1}{2}\begin{pmatrix} I & I \\ I & I \end{pmatrix}\psi, \end{aligned} \tag{2.14}$$

where

$$\gamma_5 \equiv i\gamma^0\gamma^1\gamma^2\gamma^3 = \begin{pmatrix} 0 & I \\ I & 0 \end{pmatrix}. \tag{2.15}$$

Any fermion wave functions are either LH or RH states, $\psi = \psi_{\mathrm{R}} + \psi_{\mathrm{L}}$.

The LH and RH components of the positive energy state at space-time $x = 0$ are,

$$\begin{aligned} \psi_L(0) &= \frac{1}{2}\begin{pmatrix} I & -I \\ -I & I \end{pmatrix}\sqrt{E+m}\begin{pmatrix} u \\ \eta\sigma u \end{pmatrix} = \frac{\sqrt{E+m}}{2}\begin{pmatrix} (1-\eta\sigma)u \\ -(1-\eta\sigma)u \end{pmatrix} \\ \text{and } \psi_R(0) &= \frac{1}{2}\begin{pmatrix} I & I \\ I & I \end{pmatrix}\sqrt{E+m}\begin{pmatrix} u \\ \eta\sigma u \end{pmatrix} = \frac{\sqrt{E+m}}{2}\begin{pmatrix} (1+\eta\sigma)u \\ (1+\eta\sigma)u \end{pmatrix}. \end{aligned} \tag{2.16}$$

The probability of a fermion to be LH state is,

$$P_L = \frac{|\psi_L(0)|^2}{|\psi(0)|^2} = \frac{E+m}{2}\frac{[u^\dagger(1-\eta\sigma)^2 u]}{2E|u|^2} = \frac{1}{2}(1-\beta[u^\dagger\sigma u]). \tag{2.17}$$

In the case that the velocity vector is $\beta = \beta(\sin\theta\cos\phi,\ \sin\theta\sin\phi,\ \cos\theta)$ and the spin points to $+z$ direction $u = \begin{pmatrix} 1 \\ 0 \end{pmatrix}$, the probability becomes

$$P_L = \frac{1}{2}(1-\beta\cos\theta). \tag{2.18}$$

This means that the probability is the largest when the momentum direction is opposite to the spin direction, $\theta = \pi$, and the smallest when the momentum direction is the same as the spin one, $\theta = 0$. For ultrarelativistic case, $\beta = 1$ and $P_L = \sin^2(\theta/2)$. This means that the spin direction is opposite to the momentum direction. Similarly, for the RH state of an ultrarelativistic particle, the spin is parallel to the momentum. For a particle at rest, $\beta = 0$ and $P_L = P_R = 1/2$.

Table 2.1 summarizes the relation between the helicity and relative direction of spin and momentum.

Table 2.1 The probability of LH and RH states for relative direction between the spin and momentum

P	ψ_L	ψ_R
$\mathbf{s} \parallel -\mathbf{p}$	$(1+\beta)/2$	$(1-\beta)/2$
$\mathbf{s} \parallel \mathbf{p}$	$(1-\beta)/2$	$(1+\beta)/2$

This property causes the helicity suppression of the $\pi^{\pm}$ decay. "$\mathbf{s} \parallel \mathbf{p}$" means $\mathbf{s}$ and $\mathbf{p}$ are parallel

2.2.2 Wave Function of Neutrinos

Since neutrino is massless and only LH state exists in the standard model, the neutrino wave function becomes simple. By taking $m \to 0$ in Eq. (2.13), the wave function of a positive energy massless fermion becomes,

$$\psi_{m=0}(x) = \sqrt{k} \begin{pmatrix} \hat{u} \\ \hat{\mathbf{k}}\sigma\hat{u} \end{pmatrix} e^{-i(kt-\mathbf{kx})}, \tag{2.19}$$

where $p \to (k,\ \mathbf{k})$ is the four momentum with the relation $k = |\mathbf{k}|$. The pure LH state has to satisfy

$$\gamma_R \psi_{m=0}(x) = \frac{\sqrt{k}}{2} \begin{pmatrix} (1+\hat{\mathbf{k}}\sigma)\hat{u} \\ (1+\hat{\mathbf{k}}\sigma)\hat{u} \end{pmatrix} e^{-ipx} = 0, \tag{2.20}$$

at arbitrary space-time x. Since $\hat{\mathbf{k}} = (\sin\theta\cos\phi,\ \ \sin\theta\sin\phi,\ \ \cos\theta)$,

$$(1+\hat{\mathbf{k}}\sigma)\hat{u} = \begin{pmatrix} 1+\cos\theta & e^{-i\phi}\sin\theta \\ e^{i\phi}\sin\theta & 1-\cos\theta \end{pmatrix} \hat{u} = 0. \tag{2.21}$$

This relation can be satisfied if

$$\hat{u} \propto \hat{s}(-\hat{\mathbf{k}}) = \begin{pmatrix} -ie^{-i(\phi/2)}\sin(\theta/2) \\ ie^{i(\phi/2)}\cos(\theta/2) \end{pmatrix}, \tag{2.22}$$

where $\hat{s}(\hat{\mathbf{p}})$ is the spin polarization which points toward the direction of $\mathbf{p}$. Finally the wave function of the positive energy neutrino is

$$\psi_\nu^+(x) = \sqrt{k} \begin{pmatrix} \hat{s}(-\hat{\mathbf{k}}) \\ \hat{\mathbf{k}}\sigma\hat{s}(-\hat{\mathbf{k}}) \end{pmatrix} e^{-i(kt-\mathbf{kx})}, \tag{2.23}$$

where the state propagates only forward in time. Similarly the wave function of the negative energy neutrino is

$$\psi_\nu^-(x) = \sqrt{k} \begin{pmatrix} \hat{\mathbf{k}}\sigma\hat{s}(-\hat{\mathbf{k}}) \\ \hat{s}(-\hat{\mathbf{k}}) \end{pmatrix} e^{i(kt-\mathbf{kx})}, \tag{2.24}$$

where the state propagates only backward in time and we recognize it as antineutrino.

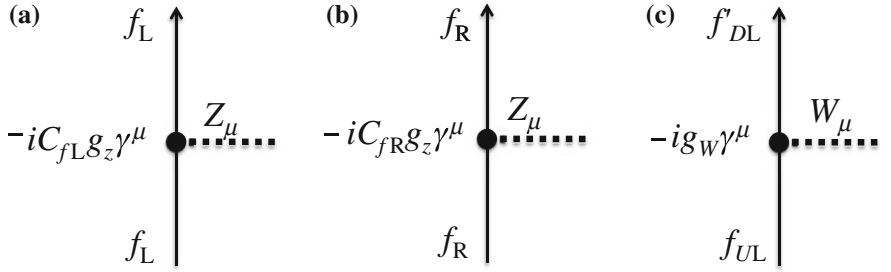

Fig. 2.2 Feynman diagram of **a** $f_L f_L Z^0$ coupling, **b** $f_R f_R Z^0$ coupling and **c** $f_U f'_D W^\pm$ coupling, where f_U is the up-type fermions and f'_D is the down-type flavor eigenstate fermions

2.3 Weak Interactions and Neutrinos

In this section, the fundamental processes of the weak interactions are described based on the standard model Lagrangian and probabilities of various neutrino interactions are calculated. The probabilities calculated here will be used later to understand neutrino oscillation experiments and their results. See also the books [2–8, Chap. 1] for details of the calculations.

2.3.1 Lagrangians for Weak Interactions

The Lagrangian of the standard model weak interaction can be obtained by setting the neutrino mixing matrix as the identical matrix in the working Lagrangian defined in Sect. 8.2. The Feynman diagrams of the weak interactions are shown in Fig. 2.2. Figure 2.2a, b shows the neutral current interactions and Fig. 2.2c shows the charged current interactions. We call $(u, c, t, \nu_e, \nu_\mu, \nu_\tau)$, up-type fermions (f_U) and (d, s, b, e, μ, τ), down-type fermions (f_D). The weak (flavor) eigenstates (d', s', b') are mixed with the mass eigenstates (d, s, b) by the Cabbibo-Kobayashi-Maskawa matrix as shown in Eq. (8.25) and f'_D is used instead of f_D when necessary.[2]

2.3.1.1 Neutral Current Interactions

The Lagrangian of the fermion f for the neutral current interactions is,

$$\mathscr{L}_{ffZ} = -iC_{fL}g_Z[\overline{f_L}\gamma^\mu f_L]Z_\mu - iC_{fR}g_Z[\overline{f_R}\gamma^\mu f_R]Z_\mu, \tag{2.25}$$

[2] For neutrinos, the flavor eigenstate and mass eigenstate are identical ($\nu' = \nu$) in the standard model and f'_D and f_D can be interpreted equivalently.

where g_Z is the coupling constant. $C_{f\mathrm{L}}$ and $C_{f\mathrm{R}}$ are coefficients for the couplings between Z^0 boson and the LH and RH components of the fermions. According to the standard model, $C_{f\mathrm{R}}$ and $C_{f\mathrm{L}}$ are given by

$$\begin{cases} C_{f_U\mathrm{R}} = -2Q_f \sin^2\theta_W \\ C_{f_U\mathrm{L}} = -2Q_f \sin^2\theta_W + 1, \end{cases} \qquad \begin{cases} C_{f_D\mathrm{R}} = -2Q_f \sin^2\theta_W \\ C_{f_D\mathrm{L}} = -2Q_f \sin^2\theta_W - 1, \end{cases} \tag{2.26}$$

where Q_f is the charge of the fermion f. θ_W is the parameter called the *weak mixing angle* or *Weinberg angle*, which is measured to be $\sin^2\theta_W \sim 0.23$.

The fermion currents in Eq. (2.25) can be modified as

$$\begin{aligned} \overline{f_\mathrm{L}}\gamma^\mu f_\mathrm{L} &= f^\dagger \gamma_\mathrm{L}^\dagger \gamma^0 \gamma^\mu \gamma_\mathrm{L} f = \overline{f}\gamma^\mu \gamma_\mathrm{L} f = \overline{f}\gamma^\mu \frac{1}{2}(1-\gamma^5) f, \\ \overline{f_\mathrm{R}}\gamma^\mu f_\mathrm{R} &= \overline{f}\gamma^\mu \gamma_\mathrm{R} f, = \overline{f}\gamma^\mu \frac{1}{2}(1+\gamma^5) f, \end{aligned} \tag{2.27}$$

and the Lagrangian (2.25) can be rewritten as

$$\mathscr{L}_{ffZ} = -ig_Z[\overline{f}\gamma^\mu \frac{1}{2}(C_{f\mathrm{V}} - C_{f\mathrm{A}}\gamma^5) f] Z_\mu, \tag{2.28}$$

where $C_{f\mathrm{V}}$ and $C_{f\mathrm{A}}$ are called the *Vector Coupling* coefficient and *Axial-vector Coupling* coefficient which are defined by

$$\begin{cases} C_{f\mathrm{V}} \equiv C_{f\mathrm{L}} + C_{f\mathrm{R}} \\ C_{f\mathrm{A}} \equiv C_{f\mathrm{L}} - C_{f\mathrm{R}} \end{cases}. \tag{2.29}$$

Contrarily, an arbitrary mixture of vector and axial vector couplings can be expressed by a combination of LH and RH couplings

$$a + b\gamma^5 = (a+b)\gamma_\mathrm{R} + (a-b)\gamma_\mathrm{L}. \tag{2.30}$$

This means that the weak and the electromagnetic interactions can be expressed by a sum of the LH and RH couplings, as well as by a sum of the vector and axial vector couplings. These coefficients are summarized in Table 2.2.

Table 2.2 Z^0-fermion coupling coefficients. $x_W = \sin^2\theta_W \sim 0.23$

Fermions	Q	C_L	C_R	C_V	C_A	$C_\mathrm{L}^2 + C_\mathrm{R}^2$
$\nu_e,\ \nu_\mu,\ \nu_\tau$	0	1	0	1	1	1
$e,\ \mu,\ \tau$	-1	$2x_W - 1$	$2x_W$	$4x_W - 1$	-1	$8x_W^2 - 4x_W + 1$
$u,\ c,\ t$	$+\frac{2}{3}$	$-\frac{4}{3}x_W + 1$	$-\frac{4}{3}x_W$	$-\frac{8}{3}x_W + 1$	1	$\frac{32}{9}x_W^2 - \frac{8}{3}x_W + 1$
$d,\ s,\ b$	$-\frac{1}{3}$	$\frac{2}{3}x_W - 1$	$\frac{2}{3}x_W$	$\frac{4}{3}x_W - 1$	-1	$\frac{8}{9}x_W^2 - \frac{2}{3}x_W + 1$

2.3.1.2 Charged Current Interactions

As for the quark-$W^{\pm}$ coupling, the Lagrangian is given by

$$\mathscr{L}_{ffW} = -ig_W[\overline{f'_{DL}}\gamma^{\mu} f_{UL}]W_{\mu} - ig_W[\overline{f_{UL}}\gamma^{\mu} f'_{DL}]W_{\mu}. \tag{2.31}$$

Finally, the Lagrangian for the electromagnetic interactions of the fermion f is

$$\mathscr{L}_{ffA} = -iQ_f e[\overline{f}\gamma^{\mu} f]A_{\mu}, \tag{2.32}$$

where A_{μ} represents the photon field. The Feynman diagram of the EM interactions is shown in Fig. 2.3. Since $Q_{\nu} = 0$ for neutrinos, they do not feel EM interactions.

Within the framework of the standard model, the weak interactions and electromagnetic interactions have the same origin and the three coupling constants, g_W, g_Z, and electric charge e, are related as,[3]

$$e = \sqrt{2}g_W \sin\theta_W = g_Z \sin 2\theta_W. \tag{2.33}$$

In general, reaction rates are proportional to powers of $(g^2/4\pi)$. Expressing the couplings in this form, the strength of the coupling between Z^0 boson and neutrinos is

$$\frac{g_Z^2}{4\pi} = \frac{\alpha}{\sin^2 2\theta_W} \sim 0.010, \tag{2.34}$$

where $\alpha \equiv e^2/4\pi \sim 0.0073$ is the electromagnetic fine structure constant. The strength of the coupling between $W^{\pm}$ boson and neutrino is

$$\frac{g_W^2}{4\pi} = \frac{\alpha}{2\sin^2\theta_W} \sim 0.016. \tag{2.35}$$

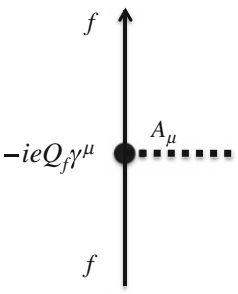

Fig. 2.3 Fermion coupling with the photon

[3] $g_W = g/\sqrt{2}$, $g_Z = g/2\cos\theta_W$, where g is the SU(2) gauge coupling constant.

Therefore, the magnitudes of the electromagnetic and weak couplings are not so different.

2.4 Neutrino Interaction Probabilities

The Lagrangians for the neutrino interactions are summarized as

$$\mathscr{L}_{\nu\nu Z} = -ig_Z \left[\overline{\nu_{lL}}\gamma^\mu \nu_{lL}\right] Z_\mu, \tag{2.36}$$

$$\mathscr{L}_{\nu l W} = -ig_W \left[\overline{l_{\mathrm{L}}}\gamma^\mu \nu_{lL}\right] W_\mu - ig_W \left[\overline{\nu_{lL}}\gamma^\mu l_{\mathrm{L}}\right] W_\mu, \tag{2.37}$$

where the wave function l stands for the charged leptons such as e, μ, τ. The Feynman diagrams which correspond to these vertexes are shown in Fig. 2.4.

The general diagram of the reaction $A + B \rightarrow A' + B'$ through intermediate gauge boson G is shown in Fig. 2.5. Its matrix element is written by

$$\mathscr{M}_{AB\rightarrow A'B'} = -g_G^2 \frac{\left[\overline{\Psi_{A'}(p_{A'})}\gamma^\mu \gamma_A \Psi_A(p_A)\right]\left[\overline{\Psi_{B'}(p_{B'})}\gamma_\mu \gamma_B \Psi_B(p_B)\right]}{q^2 - M_G^2}, \tag{2.38}$$

where g_G is the coupling constant between the fermion and the intermediate boson G, p_X is the four momenta of the fermion X, and q is the four-momentum transfer, $q = p_A - p_{A'} = p_{B'} - p_B$. M_G is the intermediate boson mass. γ_X is helicity state

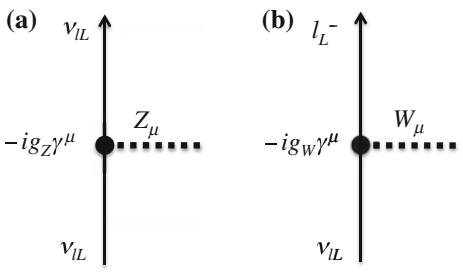

Fig. 2.4 Feynman diagram of **a** $\nu_l \nu_l Z^0$ and **b** $\nu_l l W$ couplings

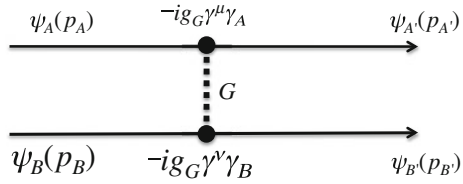

Fig. 2.5 Scattering amplitude of fermions A and B through intermediate boson G

of the coupling between fermion X and the boson G. If G is $W^{\pm}$, $\gamma_X = \gamma_{\rm L}$ and for Z^0, $\gamma_X = (C_{X\rm V} - C_{X\rm A}\gamma_5)/2$.

The wave function of each fermion is expressed as

$$\psi_X(x) = w_X e^{-ip_X x}, \tag{2.39}$$

where w_X is the four component spinor of the fermion X.
For low energy interactions, $|q^2| \ll M_G^2$, the reaction amplitude (2.38) can be expressed by the product of the spin and the exponential terms,

$$\mathscr{M}_{AB\to A'B'} = \frac{g_G^2}{M_G^2}\left[\overline{w_{A'}}\gamma_\mu\gamma_A w_A\right]\left[\overline{w_{B'}}\gamma^\mu\gamma_B w_B\right] e^{-i(p_A+p_B-p_{A'}-p_{B'})x}. \tag{2.40}$$

The exponential term becomes the delta function $\delta(p_A + p_B - p_{A'} - p_{B'})$ when integrated with respect to x, indicating the energy and momentum conservations, $p_A + p_B = p_{A'} + p_{B'}$.

The reaction probability is proportional to the absolute square of the matrix element,

$$P_{AB\to A'B'} \propto |\mathscr{M}_{AB\to A'B'}|^2 \propto G_F^2, \tag{2.41}$$

where *Fermi constant* G_F, defined by (2.42) is often used to express reaction probabilities of the weak interactions.

$$G_F = \frac{g_W^2}{2\sqrt{2}M_W^2} = \frac{g_Z^2}{\sqrt{2}M_Z^2} \sim 1.17 \times 10^{-5}[/\mathrm{GeV}^2]. \tag{2.42}$$

2.4.1 Neutrinos from Charged Pion Decay

In accelerator based neutrino experiments, the neutrinos produced in the charged pion decays are often used. The charged pion is a spin-0 pseudoscalar boson with mass $m_\pi \sim 140\,\mathrm{MeV}$. It decays with lifetime of 26 ns via the decay modes shown below,

$$\begin{aligned} \pi^{\pm} &\to \mu^{\pm} + \nu_\mu/\overline{\nu}_\mu \quad (99.99\,\%), \\ \pi^{\pm} &\to\ e^{\pm} + \nu_e/\overline{\nu}_e \quad (0.012\,\%), \end{aligned} \tag{2.43}$$

where the values in the parentheses are their branching fractions. There is a huge difference between the two branching fractions despite the lepton universality.

The Feynman diagram of the fundamental process of this decay is shown in Fig. 2.6a[4] and its physical process in the pion rest frame is shown in Fig. 2.6b. Since

[4] Actually the two quarks in the pion are in a bound state and the free wave functions can not be used. Nevertheless, this graphical view is useful to understand various properties of the pion decay.

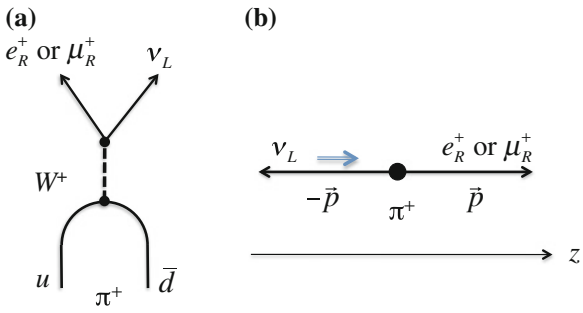

Fig. 2.6 π^+ decay. **a** A diagram. **b** Physical process in the pion rest frame. The z-axis is taken along the charged lepton's direction of motion. The neutrino moves to $-z$ and its spin points to the $+z$ direction

this is a two body decay, the final state leptons have definite energies and momentum. The energies and momentum of l and ν are[5]

$$E_\nu = \frac{m_\pi^2 - m_l^2}{2m_\pi}, \qquad E_l = \frac{m_\pi^2 + m_l^2}{2m_\pi}, \qquad p = \frac{m_\pi^2 - m_l^2}{2m_\pi}. \tag{2.44}$$

From the Feynman diagram Fig. 2.6a, the effective matrix element of this decay is,

$$\mathscr{M}_{\pi^+ \to l^+ \nu_l} \propto G_F [\overline{\nu_{lL}} \gamma^\mu l_L][\overline{d_L} \gamma_\mu u_L], \tag{2.45}$$

where l represents μ or e. The quark current is a bound system in the strong interaction potential and can be parametrized as

$$[\overline{d_L} \gamma_\mu u_L] \to f_\pi q_\mu, \tag{2.46}$$

where q_μ is the four momentum transfer and $f_\pi \sim m_\pi$ is the structure function of the pion, which corresponds to the overlapping density of the wave functions of the quarks in the pion. In the pion rest frame, $q_\mu = (m_\pi, \mathbf{0})$ and the matrix element (2.45) becomes

$$\mathscr{M}_{\pi \to l\nu} \propto G_F f_\pi m_\pi [\overline{\nu_{lL}} \gamma^0 l_L] = G_F f_\pi m_\pi [\nu_{lL}^\dagger l_L]. \tag{2.47}$$

By defining the z axis as the l^+ direction of motion as shown in Fig. 2.6b, the spinors of the neutrino and the charged lepton are,

$$\nu_{lL} = \sqrt{E_\nu} \begin{pmatrix} \chi_1 \\ -\chi_1 \end{pmatrix}, \quad l_L = \frac{\sqrt{E_l + m_l}}{2} \begin{pmatrix} -(1 - \eta_l \sigma_z)\chi_l \\ (1 - \eta_l \sigma_z)\chi_l \end{pmatrix}, \tag{2.48}$$

where χ_l represents the spin direction of the l^+ and $\eta_l = \frac{p}{E_l + m_l}$. Therefore, the matrix element (2.47) becomes

[5] If the neutrino has a finite mass m_ν, the energies and the momentum are $E_\nu = \frac{m_\pi^2 - m_l^2 + m_\nu^2}{2m_\pi}$, $E_l = \frac{m_\pi^2 + m_l^2 - m_\nu^2}{2m_\pi}$ and $p = \frac{\sqrt{((m_\pi - m_\nu)^2 - m_l^2)((m_\pi + m_\nu)^2 - m_l^2)}}{2m_\pi}$.

$$\mathscr{M}_{\pi\to l\nu} \propto G_F f_\pi m_\pi \sqrt{E_\nu (E_l + m_l)}(1-\eta_l)[\chi_1^\dagger \chi_l]. \tag{2.49}$$

In this equation only $\chi_l = \chi_1$ (the l^+ spin points in the $-z$ direction) is allowed and the matrix element becomes

$$\mathscr{M}_{\pi\to l\nu} \propto G_F f_\pi m_\pi \sqrt{E_\nu (E_l + m_l)}(1-\eta_l). \tag{2.50}$$

The decay rate is proportional to the absolute square of the matrix element,

$$\Gamma_l \propto |\mathscr{M}_{\pi\to l\nu}|^2 \propto G_F^2 f_\pi^2 (m_\pi^2 - m_l^2) m_l^2, \tag{2.51}$$

where Eqs. (2.44) are used to substitute the pion and charged lepton masses for the energies and momentum.

By taking into account the phase space, the decay rate of the pion can be calculated as [4, Chap. 1]

$$\Gamma_l = \frac{G_F^2}{8\pi} f_\pi^2 m_\pi m_l^2 \left(1 - \frac{m_l^2}{m_\pi^2}\right)^2. \tag{2.52}$$

The ratio of the decay rates of $e\nu$ and $\mu\nu$ modes is, therefore,

$$\frac{\Gamma_{\pi\to e\nu}}{\Gamma_{\pi\to\mu\nu}} = \left(\frac{m_e}{m_\mu}\right)^2 \left(\frac{m_\pi^2 - m_e^2}{m_\pi^2 - m_\mu^2}\right)^2 = 1.28 \times 10^{-4}. \tag{2.53}$$

This agrees with the observation (2.43). The fact that the decay to muons dominates makes it possible to obtain almost pure ν_μ or $\overline{\nu}_\mu$ beam in accelerator based neutrino experiments.

The mechanism to highly suppress $\pi \to e\nu$ decay is called the *helicity suppression*. Using the relation between helicity and spin polarization shown in Table 2.1, the helicity suppression can be described as follows. The produced massless neutrino is in the LH state and its spin points 100 % to $+z$ direction. Since the pion spin is 0, the only allowed charged lepton spin direction is $-z$ as shown in Fig. 2.7. On the other hand, the charged lepton is antifermion and therefore, it is in the RH state. The probability that e_R^+ spin points $-z$ is, from Table 2.1, given by

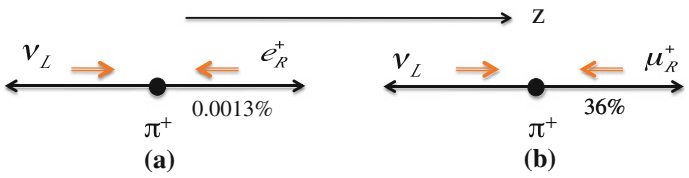

Fig. 2.7 Spin states and probabilities of **a** $\pi \to e\nu$ and **b** $\pi \to \mu\nu$ decays

$$P_{\nu e} = \frac{1-\beta_e}{2} = \frac{m_e^2}{m_\pi^2 + m_e^2} \sim 1.3 \times 10^{-5}, \tag{2.54}$$

where β_e is the velocity of the positron. Therefore, this decay channel is highly suppressed.

For $\pi \to \mu\nu$ decay, the same discussion can be applied, but the muon velocity β_μ is much smaller than β_e and the probability that μ_R^+ spin points to $-z$ is much larger,

$$P_{\nu\mu} = \frac{1-\beta_\mu}{2} = \frac{m_\mu^2}{m_\pi^2 + m_\mu^2} \sim 0.36. \tag{2.55}$$

Therefore, $\pi \to \nu\mu$ decays are not suppressed so much. Note that this suppression mechanism is not a unique property of the charged current weak interactions in which only a LH particle and a RH antiparticle can interact. It comes from the property of helicity conservation and takes place in decays of spin-0 particles with any combinations of vector and axial vector couplings.

2.4.2 Neutrinos from Muon Decay

The muons decay to

$$\begin{aligned} \mu^- &\to e^- + \nu_\mu + \bar{\nu}_e, \\ \mu^+ &\to e^+ + \bar{\nu}_\mu + \nu_e, \end{aligned} \tag{2.56}$$

with almost 100 % branching fraction. The lifetime of the muon, 2.2 μs, is much longer than the typical lifetime of other particles which decay weakly.

In some experiments, the muons are stopped in target or beam dump materials. The μ^- forms muonic atom with a nucleus in the material and quickly interact with the nucleus before it decays. On the other hand, μ^+ is repulsed from the nucleus and it decays before interacting with the nucleus. These properties can be used to obtain pure μ^+-originated neutrinos.

Since this weak decay process involves only leptons, the lifetime can be accurately calculated. From the experimental point of view, a large amount of controlled muons can be obtained and it is possible to measure its lifetime precisely. Therefore, the Fermi constant G_F has been precisely measured from the muon lifetime.

The Feynman diagram of the muon decay is shown in Fig. 2.8. The matrix element of the decay can be written from Eqs. (2.40) and (2.42) as,

$$\mathscr{M}_{\mu \to e\nu\bar{\nu}} = 2\sqrt{2} G_F [\overline{e_L} \gamma_\rho \nu_{eL}][\overline{\nu_{\mu L}} \gamma^\rho \mu_L^-]. \tag{2.57}$$

Ignoring the small m_e/m_μ terms, the calculation of the decay matrix element (2.57) shows that the energy spectrum of ν_μ is given by [2, Chap. 1] (Fig. 2.9),

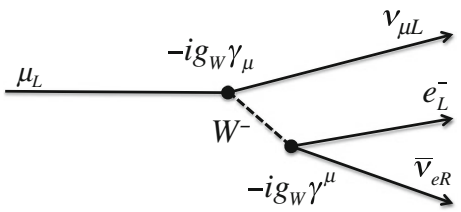

Fig. 2.8 The Feynman diagram of the muon decay

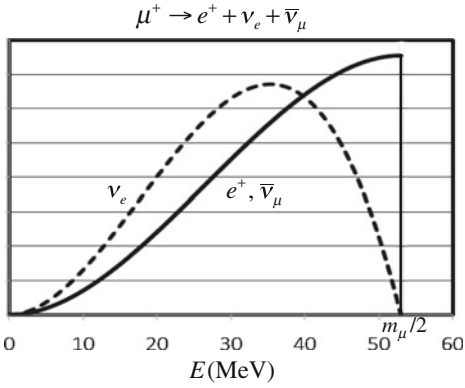

Fig. 2.9 Energy spectra of daughter particles of muon decay. m_e/m_μ terms are ignored

$$\frac{d\Gamma}{dE_{\nu_\mu}} = \frac{G_F^2 m_\mu^4}{12\pi^3}\left(\frac{E_{\nu_\mu}}{m_\mu}\right)^2\left(3 - 4\frac{E_{\nu_\mu}}{m_\mu}\right), \tag{2.58}$$

in the muon rest frame. For $\overline{\nu}_e$ and e, the energy spectra are

$$\frac{d\Gamma}{dE_{\overline{\nu}_e}} = \frac{G_F^2 m_\mu^4}{2\pi^3}\left(\frac{E_{\overline{\nu}_e}}{m_\mu}\right)^2\left(1 - 2\frac{E_{\overline{\nu}_e}}{m_\mu}\right), \tag{2.59}$$

and

$$\frac{d\Gamma}{dE_e} = \frac{G_F^2 m_\mu^4}{12\pi^3}\left(\frac{E_e}{m_\mu}\right)^2\left(3 - 4\frac{E_e}{m_\mu}\right). \tag{2.60}$$

The electron from the muon decay is called the *Michel electron*. Note that the Michel electron and muon neutrino have the same energy spectra. The angular distribution of ν_μ with respect to the muon spin is given by,

$$\frac{d\Gamma}{dx_{\nu_\mu}} = \frac{G_F^2 m_\mu^5}{6\pi^3} x_{\nu_\mu}^5\left(1 + (1 - 4x_{\nu_\mu})\cos^2\frac{\theta_{\nu_\mu}}{2}\right), \tag{2.61}$$

where $x_{\nu_\mu} = E_{\nu_\mu}/m_\mu$ and θ_{ν_μ} is the ν_μ emission angle with respect to the muon spin. For $\overline{\nu}_e$, it is

$$\frac{d\Gamma}{dx_{\bar{\nu}_e}} = \frac{G_F^2 m_\mu^5}{\pi^3} x_{\bar{\nu}_e}^2 (1 - 2x_{\bar{\nu}_e}) \cos^2 \frac{\theta_{\bar{\nu}_e}}{2}, \tag{2.62}$$

where $x_{\bar{\nu}_e} = E_{\bar{\nu}_e}/m_\mu$ and $\theta_{\bar{\nu}_e}$ is the $\bar{\nu}_e$ emission angle with respect to the muon spin.

The total decay rate is calculated by integrating one of the energy distributions (2.58)–(2.60).

$$\Gamma_\mu = \int \frac{d\Gamma}{dE} dE = \frac{G_F^2 m_\mu^5}{192\pi^3}. \tag{2.63}$$

The lifetime of the muon is the inverse of the total decay rate. From the measurements of the muon lifetime and mass, G_F is precisely determined to be

$$G_F = (1.166\,378\,7 \pm 0.000\,000\,6) \times 10^{-5}\,\text{GeV}^{-2}. \tag{2.64}$$

The G_F value can be memorized by the empirical relation, $G_F \sim (1.08)^2 \times 10^{-5}$ GeV^{-2} with a precision of 20 ppm.

2.4.3 Neutrinos from Nuclear Beta Decays

Nuclear reactors produce a huge amount of low energy $\bar{\nu}_e$'s, which have been used for various neutrino studies. The reactor neutrinos are produced in the β-decays of the unstable fission products. The fundamental reaction is the β decay of a neutron,

$$n \to p + e^- + \bar{\nu}_e. \tag{2.65}$$

The Feynman diagram of this process is shown in Fig. 2.10. This diagram is similar to the muon decay diagram shown in Fig. 2.8. However, the nucleons have internal structure and the weak coupling to the $W^\pm$ boson is modified from the muon's. The effective matrix element of the neutron β-decay can be written as

$$\mathscr{M}_\beta = \sqrt{2} G_F \cos\theta_C [\overline{e_L} \gamma^\mu \nu_{eL}][\overline{p} \gamma_\mu (1 - C_A \gamma_5) n], \tag{2.66}$$

where θ_C is the Cabbibo angle and C_A is the effective axial vector coupling coefficient of the neutron which is measured to be $C_A \sim 1.3$.

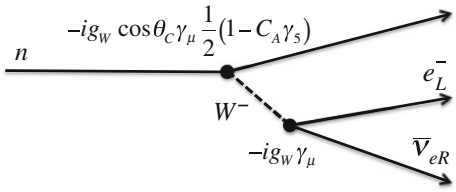

Fig. 2.10 Diagram of neutron β-decay

Using the non-relativistic reduction for the nucleon current, the squared matrix element can be expressed as

$$|\mathscr{M}_\beta|^2 = 4G_F^2 \cos^2\theta_C E_e E_\nu \left[(1+3C_A^2) + \beta_e(1-C_A^2)\cos\theta\right], \tag{2.67}$$

where θ is the angle between the electron and neutrino and $\beta_e = p_e/E_e$. The decay rate is then given by

$$\begin{aligned}\Gamma_n &= \int \frac{d^3p_e}{2E_e(2\pi)^3}\frac{d^3p_\nu}{2E_\nu(2\pi)^3}2\pi\delta(\Delta m_{np} - E_e - E_\nu)|\mathscr{M}_\beta|^2 \\ &= \frac{G_F^2\cos^2\theta_C(1+3C_A^2)}{2\pi^3}\int_{m_e}^{\Delta m_{np}} dE_e E_e p_e E_\nu p_\nu \\ &\sim \frac{1.7 m_e^5 G_F^2\cos^2\theta_C(1+3C_A^2)}{2\pi^3},\end{aligned} \tag{2.68}$$

where $\Delta m_{np} = m_n - m_p$ and the factor $1.7m_e^5$ came from the integration. The measured neutron lifetime $\tau_n = 1/\Gamma_n = 880\,\mathrm{s}$ is consistent with the expectation from the above discussions.

In nuclear β-decays, the electron in the final state is attracted by the positive charge of the final state nucleus and the decay rate is modified as follows:

$$\Gamma_A = \frac{G_F^2\cos^2\theta_C(\langle 1\rangle^2 + C_A^2\langle\sigma\rangle^2)}{2\pi^3}\int_{m_e}^{\Delta E_{if}} dE_e E_e p_e E_\nu p_\nu F(E_e, Z), \tag{2.69}$$

where $\Delta E_{if} = E_i - E_f$ and $\langle 1\rangle$ and $\langle\sigma\rangle$ terms are called the Fermi (spin non-flip) and the Gamow-Teller (spin-flip) matrix elements, respectively. $F(E_e, Z)$ corresponds to the correction factor for the final state Coulomb interactions, called the Fermi function, given by

$$F(E_e, Z) = 2(1+\xi)(2p_eR)^{2(\xi-1)}e^{\pi\zeta}\frac{|\Gamma(\xi+i\zeta)|^2}{|\Gamma(2\xi+1)|^2}, \tag{2.70}$$

where R is the radius of the nucleus, $\xi = \sqrt{1-\alpha^2Z^2}$ and $\zeta = \frac{Z\alpha E_e}{p_e}$. The Fermi function can be simplified for the nonrelativistic case as

$$F(E, Z) \sim \frac{2\pi\zeta}{1-e^{-2\pi\zeta}}. \tag{2.71}$$

The neutrino energy spectrum is, then,

$$\frac{d\Gamma_A}{dE_\nu} \propto E_\nu^2(\Delta E_{if} - E_\nu)\sqrt{(\Delta E_{if} - E_\nu)^2 - m_e^2}F(E_e, Z). \tag{2.72}$$

2.4.4 νe^- Scatterings

The neutrino-electron elastic scatterings are used for detection of solar neutrinos. In this section, those scattering cross sections are reviewed.

The description starts with $\nu_\mu e^-$ scattering since it involves a single reaction diagram. Then the other scattering cross sections are calculated making use of the formula developed for the $\nu_\mu e^-$ scattering. Those scattering processes include only leptons and the cross sections can be calculated precisely.

2.4.4.1 $\nu_\mu + e^- \to \nu_\mu + e^-$ Scattering

The Feynman diagram of $\nu_\mu + e^- \to \nu_\mu + e^-$ scattering process is shown in Fig. 2.11. The target electron is supposed to be at rest. The matrix element of the scattering is, from (2.40), given by

$$\begin{aligned}\mathscr{M}_{\nu_\mu e} &= 2\sqrt{2}G_F[\overline{\nu_{\mu L}(k_f)}\gamma_\rho \nu_{\mu L}(k_i)][\overline{e(p_e)}\gamma^\rho(C_{eL}\gamma_L + C_{eR}\gamma_R)e(m_e,\mathbf{0})] \\ &= 2\sqrt{2}G_F[\overline{\nu_{\mu L}}\gamma_\rho \nu_{\mu L}]\left(C_{eL}[\overline{e_L}\gamma^\rho e_L] + C_{eR}[\overline{e_R}\gamma^\rho e_R]\right),\end{aligned} \tag{2.73}$$

where the $e - Z^0$ coupling coefficients are, from Table 2.2,

$$C_{eR} = 2\sin^2\theta_W, \quad C_{eL} = -1 + 2\sin^2\theta_W, \tag{2.74}$$

respectively. The cross section is proportional to the absolute square of the scattering amplitude and is expressed by

$$\sigma_{\nu e} \propto C_{eL}^2((k_f+p_e)^2-m_e^2)^2 + C_{eR}^2((k_i-p_e)^2-m_e^2)^2 + C_{eL}C_{eR}m_e^2(k_f-k_i)^2. \tag{2.75}$$

From the detailed calculation, the differential cross section is given by

$$\frac{d\sigma_{\nu_\mu e}}{dy} = \sigma_{\nu e}^0(k_i)\left(C_{eL}^2 + C_{eR}^2(1-y)^2 - C_{eL}C_{eR}\varepsilon y\right), \tag{2.76}$$

where T_e is the kinetic energy of the recoiled electron, $y = T_e/k_i$ and $\varepsilon = m_e/k_i$. $\sigma_{\nu e}^0(k_i)$ is a reference νe scattering cross section expressed by

$$\sigma_{\nu e}^0(k_i) \equiv \frac{2G_F^2 m_e k_i}{\pi} \sim 1.7\times 10^{-44}(k_i/\mathrm{MeV})\ \mathrm{cm}^2. \tag{2.77}$$

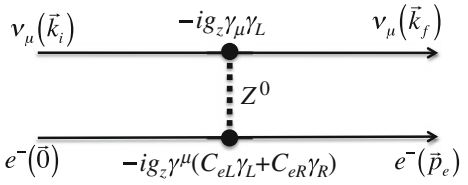

Fig. 2.11 Feynman diagram of $\nu_\mu e^-$ scattering

The total cross section can be calculated by integrating the differential cross section (2.76) and is given by

$$\sigma_{\nu_\mu e} = \int_0^{y_{\rm MAX}} \frac{d\sigma_{\nu_\mu e}}{dy} dy = \sigma^0_{\nu e}(k_i) \left(C^2_{e\rm L} + \frac{1}{3} C^2_{e\rm R} - \frac{1}{2} C_{e\rm L} C_{e\rm R} \varepsilon \right), \tag{2.78}$$

where $y_{\rm MAX} = \frac{1}{1+(m_e/2k_i)}$ corresponds to the maximum kinetic energy that the recoil electron can have. If we ignore the third term in (2.78), the total cross section is approximately given by

$$\sigma_{\nu_\mu e} = 1.55 \times 10^{-45} (k_i/{\rm MeV})\ {\rm cm}^2. \tag{2.79}$$

The cross section is proportional to the incident neutrino energy k_i.

Since the electron density in the water is $\sim 3 \times 10^{23}/{\rm cm}^3$, the mean free path of 10 MeV neutrinos for $\nu_\mu - e$ scattering in water is two light years.

2.4.4.2 $\bar{\nu}_\mu + e^- \to \bar{\nu}_\mu + e^-$ Scattering

Figure 2.12 shows the Feynman diagram of $\bar{\nu}_\mu e^-$ scattering. Since only $\bar{\nu}_{\mu R}$ interacts, the matrix element of the scattering is written by

$$\mathscr{M}_{\bar{\nu}_\mu e} = 2\sqrt{2} G_F [\overline{\bar{\nu}_{\mu\rm R}} \gamma_\rho \bar{\nu}_{\mu\rm R}] (C_{e\rm L} [\overline{e_{\rm L}} \gamma^\rho e_{\rm L}] + C_{e\rm R} [\overline{e_{\rm R}} \gamma^\rho e_{\rm R}]). \tag{2.80}$$

The antineutrino wave function in Eq. (2.80) can be rewritten using the negative energy neutrino wave function as follows:

$$\mathscr{M}_{\bar{\nu}_\mu e} = 2\sqrt{2} G_F [\overline{\nu_{\mu\rm L}(-k_i)} \gamma_\rho \nu_{\mu\rm L}(-k'_f)] \left(C_{e\rm L} [\overline{e_{\rm L}} \gamma^\rho e_{\rm L}] + C_{e\rm R} [\overline{e_{\rm R}} \gamma^\rho e_{\rm R}] \right). \tag{2.81}$$

This amplitude is obtained by the substitution of the neutrino momentum $k_f \leftrightarrow -k_i$ in Eq. (2.73). Therefore, the cross section for the matrix element (2.80) can also be obtained from the same substitution in the $\nu_\mu e$ cross section formula of (2.75):

$$\sigma_{\bar{\nu}_\mu e} \propto C^2_{e\rm L} ((p_e - k_i)^2 - m_e^2)^2 + C^2_{e\rm R} ((k_f + p_e)^2 - m_e^2)^2 + C_{e\rm L} C_{e\rm R} m_e^2 (k_f - k_i)^2. \tag{2.82}$$

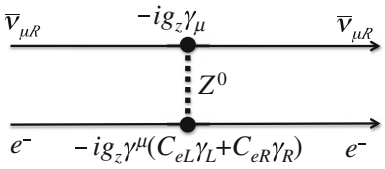

Fig. 2.12 Feynman diagram of $\bar{\nu}_\mu e^-$ scattering

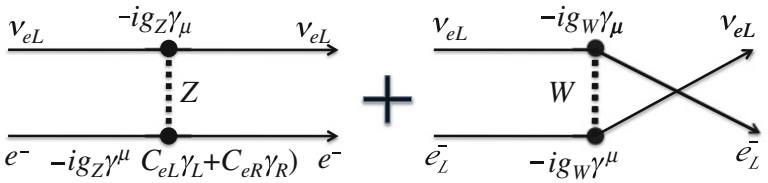

Fig. 2.13 The Feynman diagram of $\nu_e e^-$ scattering. The neutral and charged current diagrams have to be added

This is exactly the same formula obtained by substituting $C_{e\mathrm{R}} \leftrightarrow C_{e\mathrm{L}}$ in (2.75). Therefore, the form of the $\bar{\nu}_\mu e^-$ cross section is equivalent to the forms of the $\nu_\mu e^-$ cross section, (2.76) and (2.78), after substituting

$$(C_{e\mathrm{L}},\ C_{e\mathrm{R}}) \ \rightarrow \ (C_{e\mathrm{R}},\ C_{e\mathrm{L}}). \tag{2.83}$$

2.4.4.3 $\nu_e + e^- \rightarrow \nu_e + e^-$ Scattering

For the $\nu_e e^-$ scattering, the contribution from the charged current scattering has to be added to the neutral current scattering amplitude as shown in Fig. 2.13. The matrix element of this scattering is then given by

$$\mathscr{M}_{\nu_e e} = 2\sqrt{2}G_F\left([\overline{\nu_{eL}}\gamma_\rho\nu_{eL}]\left(C_{e\mathrm{L}}[\overline{e_\mathrm{L}}\gamma^\rho e_\mathrm{L}] + C_{e\mathrm{R}}[\overline{e_\mathrm{R}}\gamma^\rho e_\mathrm{R}]\right) - [\overline{e_\mathrm{L}}\gamma_\rho\nu_{eL}][\overline{\nu_{eL}}\gamma^\rho e_\mathrm{L}]\right), \tag{2.84}$$

where the relative minus sign in the charged current term comes from the exchange of the two leptons. Making use of the Fierz identity,[6]

$$[\overline{e_\mathrm{L}}\gamma_\rho\nu_{eL}][\overline{\nu_{eL}}\gamma^\rho e_\mathrm{L}] = -[\overline{\nu_{eL}}\gamma_\rho\nu_{eL}][\overline{e_\mathrm{L}}\gamma^\rho e_\mathrm{L}], \tag{2.85}$$

equation (2.84) can be factorized as

$$\mathscr{M}_{\nu_e e} = 2\sqrt{2}G_F[\overline{\nu_{eL}}\gamma_\rho\nu_{eL}]\left((C_{e\mathrm{L}}+1)[\overline{e_\mathrm{L}}\gamma^\rho e_\mathrm{L}] + C_{e\mathrm{R}}[\overline{e_\mathrm{R}}\gamma^\rho e_\mathrm{R}]\right). \tag{2.86}$$

Therefore, the cross section can be obtained by substituting

$$(C_{e\mathrm{L}},\ C_{e\mathrm{R}}) \ \rightarrow \ (C_{e\mathrm{L}}+1,\ C_{e\mathrm{R}}), \tag{2.87}$$

in Eqs. (2.76) and (2.78).

[6] See Sect. 8.1.6 and the solution of the Problem 13.9 in [4, Chap. 1].

2.4.4.4 $\bar{\nu}_e + e^- \to \bar{\nu}_e + e^-$ Scattering

The Feynman diagram for $\bar{\nu}_e e^-$ scattering is shown in Fig. 2.14. The matrix element of the scattering is given by

$$\mathscr{M}_{\bar{\nu}_e e} = 2\sqrt{2}G_F\Big([\overline{\bar{\nu}_{eR}}\gamma_\rho\bar{\nu}_{eR}](C_{eL}[\overline{e_L}\gamma^\rho e_L] + C_{eR}[\overline{e_R}\gamma^\rho e_R]) - [\overline{e_L}\gamma_\rho\bar{\nu}_{eR}][\overline{\bar{\nu}_{eR}}\gamma^\rho e_L]\Big). \tag{2.88}$$

As in the previous subsection, this amplitude can be rewritten using the negative energy neutrino wave function.

$$\mathscr{M}_{\bar{\nu}_e e} = 2\sqrt{2}G_F\left\{\begin{array}{l}[\overline{\nu_{eL}(-k_i)}\gamma_\rho\nu_{eL}(-k_f)]\left(C_{eL}[\overline{e_L}\gamma^\rho e_L] + C_{eR}[\overline{e_R}\gamma^\rho e_R]\right)\\ +[\overline{e_L}\gamma_\rho\nu_{eL}(-k_f)][\overline{\nu_{eL}(-k_i)}\gamma^\rho e_L]\end{array}\right\}. \tag{2.89}$$

Applying the Fierz identity again,

$$\mathscr{M}_{\bar{\nu}_e e} = 2\sqrt{2}G_F[\overline{\nu_{eL}(-k_i)}\gamma_\rho\nu_{eL}(-k_f)]\left((C_{eL}+1)[\overline{e_L}\gamma^\rho e_L] + C_{eR}[\overline{e_R}\gamma^\rho e_R]\right). \tag{2.90}$$

The cross section can be obtained by substituting

$$(C_{eL},\ C_{eR}) \ \to\ (C_{eR},\ C_{eL}+1), \tag{2.91}$$

in Eqs. (2.76) and (2.78).

2.4.4.5 Summary of νe Scattering Cross Sections

As we saw, various neutrino-electron scattering modes can be treated with the same formula. The difference is the coefficients of the electron currents. In summary, the general νe scattering cross section forms for $d\sigma_{\nu e}/dy$ and $\sigma_{\nu e}$ are

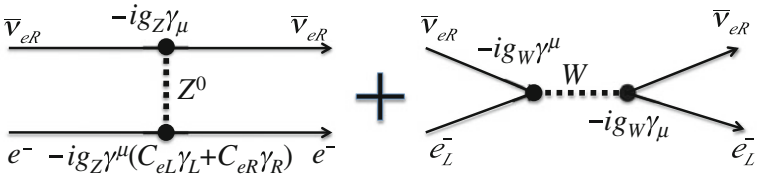

Fig. 2.14 The Feynman diagram of $\bar{\nu}_e e^-$ scattering. The neutral and charged current diagrams have to be added

$$\begin{aligned}\frac{d\sigma_{\nu e}}{dy} &= \sigma^0_{\nu e}(k_i)\left(g_{\rm L}^2 + g_{\rm R}^2(1-y)^2 - g_{\rm L}g_{\rm R}\varepsilon y\right),\\ \sigma_{\nu e} &= \sigma^0_{\nu e}(k_i)\left(g_{\rm L}^2 + \frac{1}{3}g_{\rm R}^2 - \frac{1}{2}g_{\rm L}g_{\rm R}\varepsilon\right).\end{aligned} \tag{2.92}$$

The reference νe cross section $\sigma^0_{\nu e}(k_i)$ is shown in Eq. (2.77). The effective coupling coefficients $g_{\rm L/R}$ for various νe scattering modes are summarized in Table 2.3. The energy spectra of the νe scatterings for $k_i = 10\,\text{MeV}$ neutrinos are shown in Fig. 2.15.

The numerical total cross sections for the νe scatterings are summarized in Eq. (2.93).

$$\begin{cases}\sigma_{\nu_\mu e^-} = \sigma_{\nu_\tau e^-} \sim 1.55\times 10^{-45}(k_i/\text{MeV})\ \text{cm}^2,\\ \sigma_{\bar\nu_\mu e^-} = \sigma_{\bar\nu_\tau e^-} \sim 1.34\times 10^{-45}(k_i/\text{MeV})\ \text{cm}^2,\\ \sigma_{\nu_e e^-} \sim 9.52\times 10^{-45}(k_i/\text{MeV})\ \text{cm}^2,\\ \sigma_{\bar\nu_e e^-} \sim 3.99\times 10^{-45}(k_i/\text{MeV})\ \text{cm}^2.\end{cases} \tag{2.93}$$

Table 2.3 Z^0-fermion coupling coefficients $x_W = \sin^2\theta_W \sim 0.23$ is used for the numerical calculations

Mode	$g_{\rm L}$	$g_{\rm R}$	$g_{\rm L}^2 + \frac{1}{3}g_{\rm R}^2$	$\frac{1}{2}g_{\rm L}g_{\rm R}$
$\nu_\mu e^-,\ \nu_\tau e^-$	$-1+2x_W$	$2x_W$	0.36	0.12
$\bar\nu_\mu e^-,\ \bar\nu_\tau e^-$	$2x_W$	$-1+2x_W$	0.31	0.25
$\nu_e e^-$	$1+2x_W$	$2x_W$	2.1	0.34
$\bar\nu_e e^-$	$2x_W$	$1+2x_W$	0.93	0.34

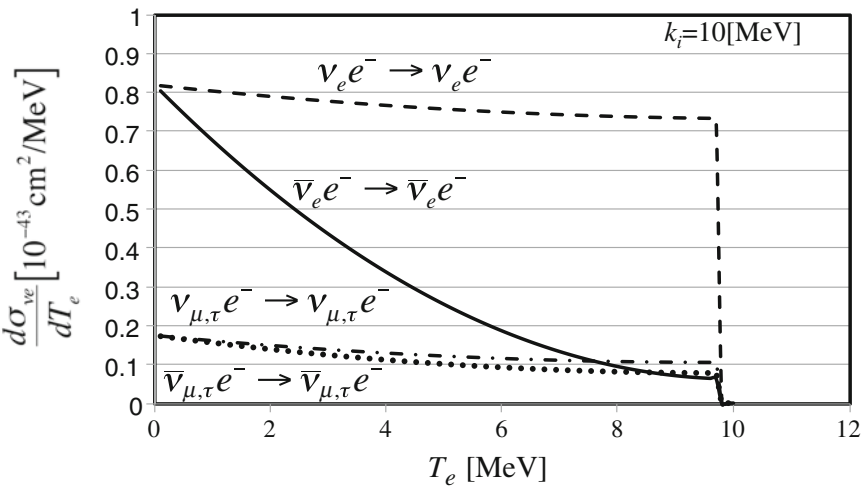

Fig. 2.15 Energy spectra of νe^- scatterings for incident neutrino energy $k_i = 10\,\text{MeV}$

Since there is the following relation between the electron scattering angle and kinetic energy,

$$T_e = m_e \frac{2\cos^2\theta}{\varepsilon(2+\varepsilon)+\sin^2\theta}, \tag{2.94}$$

the differential cross section as a function of the scattering angle is

$$\frac{d\sigma_{\nu e}}{d\cos\theta_e} = 4\sigma^0_{\nu e}\varepsilon(1+\varepsilon)^2 \times \cos\theta(F(\theta))^2(g_{\mathrm{L}}^2 + g_{\mathrm{R}}^2(1-2\varepsilon\cos^2\theta F(\theta))^2 - 2g_{\mathrm{L}}g_{\mathrm{R}}\varepsilon^2\cos^2\theta F(\theta)), \tag{2.95}$$

where

$$F(\theta) = \frac{1}{\varepsilon(\varepsilon+2)+\sin^2\theta}. \tag{2.96}$$

For $k_i \gg m_e$, the electrons are scattered forward with width of $\delta\theta \sim \sqrt{\varepsilon}$. Figure 2.16 shows the $\cos\theta$ distribution of the scattered electron for $k_i = 5$ and 10 MeV.

2.4.5 *Inverse* β *Decay*

The inverse process of the β decay,

$$\bar{\nu}_e + {}^{Z}A \rightarrow e^+ + {}^{(Z-1)}A, \tag{2.97}$$

is called the *inverse* β *decay* (IBD) reaction. The IBD reaction for the proton target,

$$\bar{\nu}_e + p \rightarrow e^+ + n, \tag{2.98}$$

is often used to detect reactor neutrinos. The cross section of the low energy IBD reaction is more accurately known than those of other neutrino-nucleus interactions.

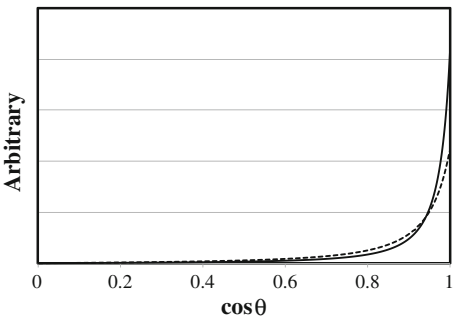

Fig. 2.16 The $\cos\theta$ distribution of electron in νe scattering. The *solid line* is for $k_i = 10$ MeV and the *dashed line* is for $k_i = 5$ MeV

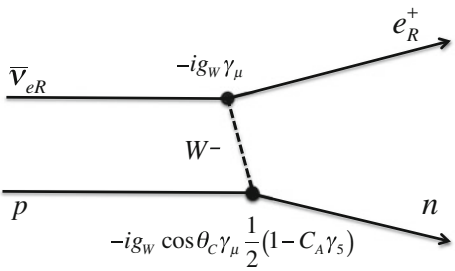

Fig. 2.17 Diagram of the inverse beta decay reaction

Figure 2.17 shows the diagram of the IBD reaction. The matrix element of the IBD reaction can be written as the same form as Eq. (2.66) and is given by

$$\mathscr{M}_{\mathrm{IBD}} = \sqrt{2}G_F \cos\theta_{\mathrm{C}}[\overline{e_{\mathrm{L}}}\gamma^{\mu}\nu_{e\mathrm{L}}][\overline{n}\gamma_{\mu}(1 - C_{\mathrm{A}}\gamma_5)p]. \tag{2.99}$$

From this matrix element and the neutron decay width (2.68), the IBD cross section can be related to the neutron lifetime τ_n as

$$\begin{aligned}\sigma_{\mathrm{IBD}}(E_\nu) &= \frac{G_F^2(1+3C_{\mathrm{A}}^2)\cos^2\theta_{\mathrm{C}}}{\pi}E_e p_e = \frac{2\pi^2}{1.7m_e^5\tau_n}E_e p_e \\ &\sim 1.0\times 10^{-43}(E_\nu - \Delta m_{np})\sqrt{(E_\nu - \Delta m_{np})^2 - m_e^2}\ \ \mathrm{cm}^2,\end{aligned} \tag{2.100}$$

where the masses and energies are expressed in MeV and $\Delta m_{np} = m_n - m_p = 1.29\,\mathrm{MeV}$. The energy dependence of the cross section is shown in Fig. 5.32. The momentum transfer is small for reactor neutrino detection, since the typical neutrino energy is ~4 MeV. Therefore, radiative and recoil corrections are small and the uncertainty is dominated by the error of the neutron lifetime measurement.

http://www.springer.com/978-4-431-55461-5

Neutrino Oscillations
A Practical Guide to Basics and Applications
Suekane, F.
2015, XIV, 185 p. 88 illus., 42 illus. in color., Softcover
ISBN: 978-4-431-55461-5